Bull. Korean Soc. Fish. Tech. 36(2), 2000 韓國漁業技術學會誌, 36(2), 2000

Evaluation of the Fatigue Behavior before and after Wall Thickness Penetration in Carbon Steel Pipes with Circumferential Part Through-Wall Surface Crack

Seok-Hwan AHN

Pukyong National University

(Received May 19, 2000)

원주방향 미관통 표면결함을 가지는 탄소강 배관의 두께관 통전·후의 피로거동 평가

안 석 환

부경대학교

(2000년 5월 19일 접수)

요 약

실온 대기 중에서 탄소강배관(STS370)의 피로시험을 행하였다. 배관에는 외부결함을 인공적으로 상정하여, 피로균열진전 및 관통의 거동, 균열형상, 누설 및 파단수명, 균열개구변위를 실험과 이론의 양면으로부터 비교·검토하였다. 특히, 배관의 벽두께 관통후에 있어서의 응력확대계수를 평가하기 위하여 새로운 식을 제안하였다. 피로균열이 관벽을 관통하기 전에 있어서는 판모델에 의한 Newman-Raju의 응력확대계수 평가식을 이용하므로서 aspect 비와 누설수명 등 관통전의 피로균열성장거동을 평가할 수 있음을 나타내었다. 또한, 피로균열이 관벽을 관통한 후에 있어서는 본 논문에서 제안한 배관모델에 의한 응력확대계수의 평가식을 이용하여 관통후의 균열형상, 파단수명 및 균열개구변위 등 관통후의 피로균열성장거동을 평가하였다.

INTRODUCTION

The Leak Before Break (*LBB*) design philosophy used for nuclear power plants and storage tanks has recently been attracting much attention from a safety and economic point of view. The most important steps which should be investigated in a *LBB* design can be summarized as follows[1] : (a) throughout the life, a crack should not occur ; (b) if a crack occurs, the crack propagation should be small and detectable in order to be repaired during regular inspection ; (c) if a crack occurs and penetrates the structural parts, the crack propagation and the leakage should be as small as possible.

Studies of *LBB* designs have been performed on various aspects of steps (a) and (b) above[2]. There have also been some studies on step (c) and some useful knowledge about the effects of surface cracks has been reported[3]. The present authors have reported a systematic investigation on the *LBB* condition, crack growth behavior and crack opening behavior of a plate

under a fatigue stress[4]. Studies of crack propagation behavior and the crack opening displacement on a complex through crack after penetration of the pipe, however, are relatively rare[5]. It is, therefore, difficult to evaluate quantitatively fatigue crack behavior after penetration of the pipe.

For that reason, the present authors have proposed a simplified evaluation model for determining the stress intensity factor after penetration. It was found that the crack propagation characteristics, the crack shape change and the crack opening displacement after penetration in a pipe can be evaluated quantitatively by using the proposed equation and pipe model.

EVALUATION OF STRESS INTENSITY FACTORS

The stress intensity factor before penetration was estimated by using the plate medel and Newman-Raju formula[6]. The plate model is shown in Figure 1(a). In this plate model, the following assumption was made : plate width is $2\pi R_S$, plate thickness is t, surface crack length is $2C_S$, crack depth is a and the plate is subjected to a tensile stress equal to bending stress σ_B.

The stress intensity factors K_S and K_B at points S and B(Fig. 1(b)) after penetration were evaluated by the equation proposed by the present authors. When deriving the above K equations, four assumptions were made:

(A) After crack penetration, a crack is located symmetrically around the maximum tension point, Stresses were calculated elastically and a crack angle θ_M on the midsection is given by the following equation :

$$\theta_M=(\theta_S+\theta_b)/2 \qquad (1)$$

(B) The crack opening displacement at the center of the crack after penetration(on the line XX′ in Fig. 1(b)) is assumed to be the same on the outer surface and the inner surface.

(C) The crack opening displacement $\delta(\theta_M)$ at the center of the wall thickness of a pipe (on the line XX' in Fig. 1(b)) is assumed to be the same as the crack opening displacement at the center of a simple through wall crack ($\theta_S=\theta_b$) with a crack angle $2\theta_M$ in a pipe. Hence $\delta(\theta_M)$ can be expressed as follows[7] :

$$\delta(\theta_M)=4\sigma_B \cdot \{R_S-(t/2)\}\ \theta_M \cdot V_b/E \qquad (2)$$

where :

$$V_b=1+A\{6.071(\theta_M/\pi)^{1.5}+24.15(\theta_M/\pi)^{2.94}\}$$
$$A=[0.125\{(R_S-(t/2))/t\}-0.25]^{0.25}$$
$$(valid\ range\ : 3.5\leq\{(R_S-(t/2))/t\}\leq 10) \qquad (3)$$

(D) The stress intensity factors K_S and K_B at points S and B(Fig. 1(b)) after penetration are assumed to be equal to the stress intensity factor, whereby the crack opening displacement at the center of crack angle $2\theta_S$ or $2\theta_b$ of pipe is exposed to the elastic bending stress corresponding to $\delta(\theta_M)$.

These four assumptions make it possible to express the stress intensity factors for a complex through wall crack ($\theta_S\geq\theta_b$) such as

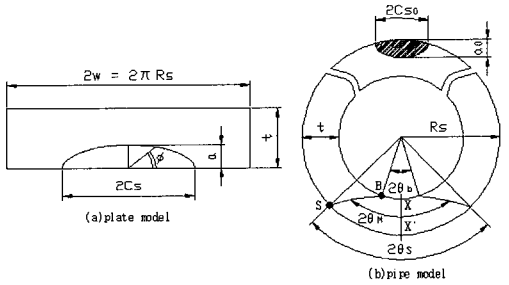

Fig. 1. Model to evaluate stress intensity factor before and after crack penetration : (a) plate model, (b) pipe model.

points S and B in Figure 1b by using the K formula for a simple through wall crack[7] :

$$K_S=K(\theta_S)=\delta(\theta_M)/\delta(\theta_S)\cdot\sigma_B\cdot[\pi\{R_S-(t/2)\}\theta_S]^{0.5}\cdot F_b(\theta_S)$$
$$K_B=K(\theta_b)=\delta(\theta_M)/\delta(\theta_b)\cdot\sigma_B\cdot[\pi\{R_S-(t/2)\}\theta_b]^{0.5}\cdot F_b(\theta_b) \quad (4)$$

where :

$$F_b(\theta_S)=1+A\{4.5967(\theta_S/\pi)^{1.5}+2.6422(\theta_S/\pi)^{4.24}\}$$
$$F_b(\theta_b)=1+A\{4.5967(\theta_b/\pi)^{1.5}+2.6422(\theta_b/\pi)^{4.24}\} \quad (5)$$

$\delta(\theta_S)$ and $\delta(\theta_b)$ are found by substituting θ_S or θ_b for θ_M in Equation (2), and $V_b(\theta_S)$ and $V_b(\theta_b)$ by substituting θ_S or θ_b for θ_M in Equation (3).

MATERIALS AND TESTING PROCEDURE

The pipe used in this study was the carbon steel pipe of *STS370*. The mechanical properties and the chemical composition are given by the following Table 1 and 2.

Figure 1(b) shows the geometry of the pipe tested. The notch of surface length $2C_{SO}$ and depth a_0 was located on the outer surface of the specimens using an electric discharge machine or saw. The specimens details and test conditions are shown in Table 3. The fatigue tests were made at room temperature using an electrohydraulic fatigue testing machine with a capacity of 196 kN. A four points bending test system with outer span $L_0=1000$ mm and inner span $L_1=245$ mm was adopted. Fatigue tests were carried out under load control. The test conditions were : sine wave loading, frequency 1-5 Hz, and stress ratio $R=0.1$. The crack length $2C_S$ (Fig. 1) on the outer surface was measured using a stereomicroscope. The crack depth a and the inner crack length $2C_b$ on the penetrated surface were measured after fracture by the beach mark method. All of the beach mark load cycles were conducted at a R ratio of 0.1 and a frequency of 10 Hz. Crack opening displacement(COD) was measured by a clip gauge.

Table 1. Mechanical properties of tested materials

Material	Tensile strength (*MPa*)	Yield strength (*MPa*)	Elongation (%)
STS370	406	227	25.3

Table 2. Chemical compositions of tested materials [wt %]

Material	C	Si	Mn	P	S
STS370	0.15	0.25	0.43	0.008	0.007

Table 3. Specimen geometries and test results

Specimen No.	Specimen Geometry					Stress Condition		N_L (Cycle)	N_F (Cycle)
	$2C_{SO}$ (*mm*)	a_0 (*mm*)	R_S (*mm*)	t (*mm*)	$2\theta_0$ (°)	σ_{MAX} (*MPa*)	σ_{MIN} (*MPa*)		
FB−1	44.9	4.5	51.0	8.5	50.4	196.0	19.60	14887	35929
FB−2	44.0	4.5	〃	〃	49.4	325.9	32.59	—	—
FB−3	36.5	3.0	〃	〃	41.0	196.0	19.60	32381	47521
FB−4	12.0	3.0	〃	〃	13.6	325.9	32.59	21187	26940
FB−5	12.0	3.0	〃	〃	13.6	196.0	19.60	220671	261321
FB−6	8.0	2.0	〃	〃	9.0	325.9	32.59	52910	58150
FB−7	35.8	3.0	〃	〃	40.2	257.2	25.72	15367	23281
FB−8	65.0	10.0	〃	12.7	73.0	98.0	9.80	123510	370780
FB−9	12.0	6.0	〃	〃	13.6	147.0	14.70	990451	1102678
FB−10	18.0	4.5	〃	〃	20.2	239.6	23.96	88900	128267

TEST RESULTS AND CONSIDERATION

1. Crack growth behavior before crack penetration

The fatigue fracture surfaces obtained from experiment are shown in Figure 2. Figures 2(a) and 2(c) show the results obtained from the specimens subjected to low cyclic bending stress. Figure 2(b) and 2(d) show the results obtained from the specimen subjected to high cyclic bending stress. Aspect ratios of the fatigue crack were evaluated from these photographs. A comparison between the measured aspect ratios and the calculated ones is shown in Figure 3(a) and (b). From this figure, the following three characteristics can be noted : 1) The calculated aspect ratios show good agreement with the experimental ones regardless of initial aspect ratio, bending stress level and wall thickness. 2) When initial aspect ratio is small, it increases with crack

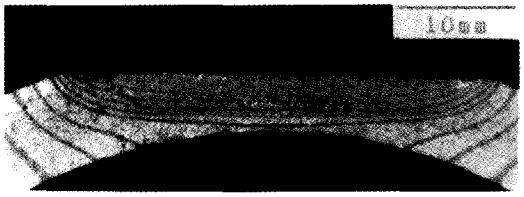

(a) FB−3
($2C_{S0}$=36.5mm, a_0=3.0mm, σ_B=196.0Mpa)

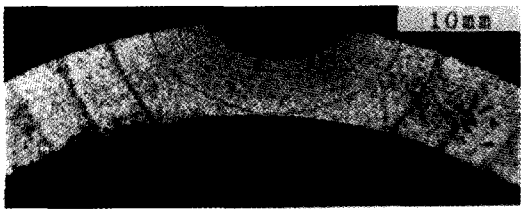

(b) FB−4
($2C_{S0}$=12.0mm, a_0=3.0mm, σ_B=325.9Mpa)

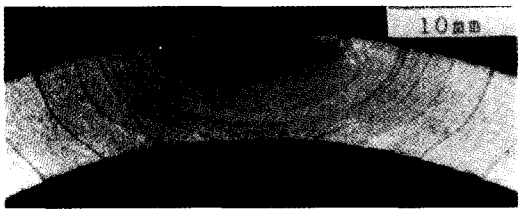

(c) FB−5
($2C_{S0}$=12.0mm, a_0=3.0mm, σ_B=196.0Mpa)

(d) FB−10
($2C_{S0}$=18.0mm, a_0=4.5mm, σ_B=239.6Mpa)

Fig. 2. Fatigue fracture surface and beach marks.

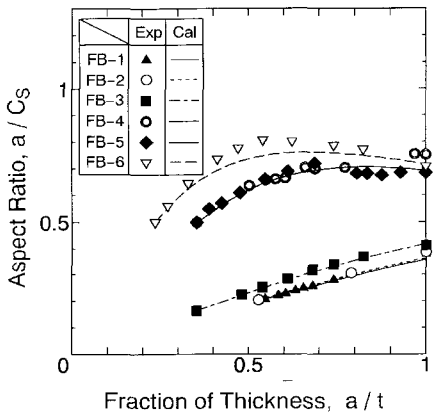

(a)

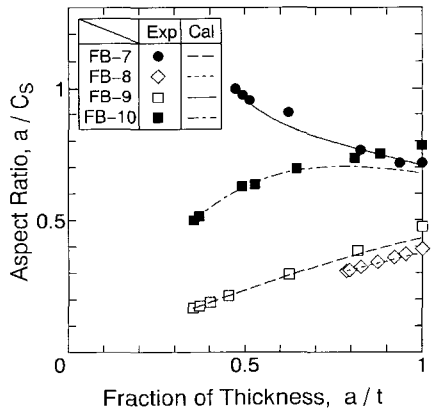

(b)

Fig. 3. Calculated and measured aspect ratio vs *a/t*.

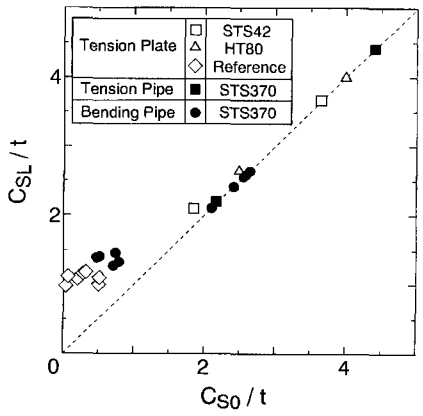

Fig. 4. Correlation between C_{SL}/t and initial C_{SO}/t.

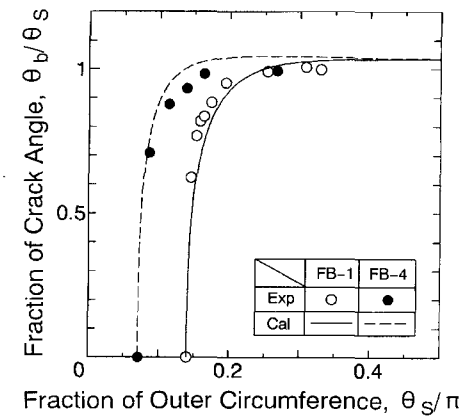

(a)

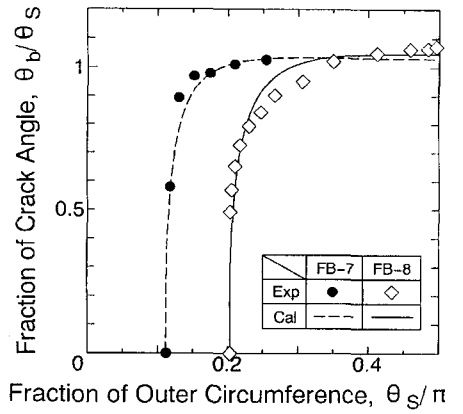

(b)

Fig. 5. Comparison between experimental and calculated crack shape after penetration.

growth. However, for case of a large initial aspect ratio, it shows a convex curve and the maximum values on the way. 3) The calculated aspect ratio at crack penetration, which is very important for *LBB* design, shows good agreement with the experimental one.

Fatigue crack shape at crack penetration is an important factor in *LBB* design. The correlation between the surface crack length at crack penetration (C_{SL}) and the initial surface crack length (C_{SO}) is shown in Figure 4. From this figure, it can be seen that when C_{SO}/t is lower than about 1.5, C_{SL}/t shows an almost constant value of 1.5. However, when C_{SO}/t is greater than about 1.5, C_{SL}/t and C_{SO}/t indicate almost the same value regardless of the load conditions and the materials.

2. Crack growth behavior after crack penetration

Fatigue crack shape and fatigue life after crack penetration are also important factors for *LBB* design. Figure 5(a) and (b) show the correlation between the experimental crack angle ratio θ_b/θ_S (Fig. 1(b)) measured in Figure 2 and the calculated one. From this figure, it can be seen that for the first stage after crack penetration, the inner crack angle θ_b becomes equal to the outer crack angle θ_s. The correlation between the experimental and calculated values of θ_b/θ_S show very good agreement despite the bending stress level and crack size at penetration.

3. Fatigue crack growth rate and stress intensity factor

For the calculation of fatigue crack growth rate da/dN, the number of cycles before the first beach mark was neglected in order to eliminate

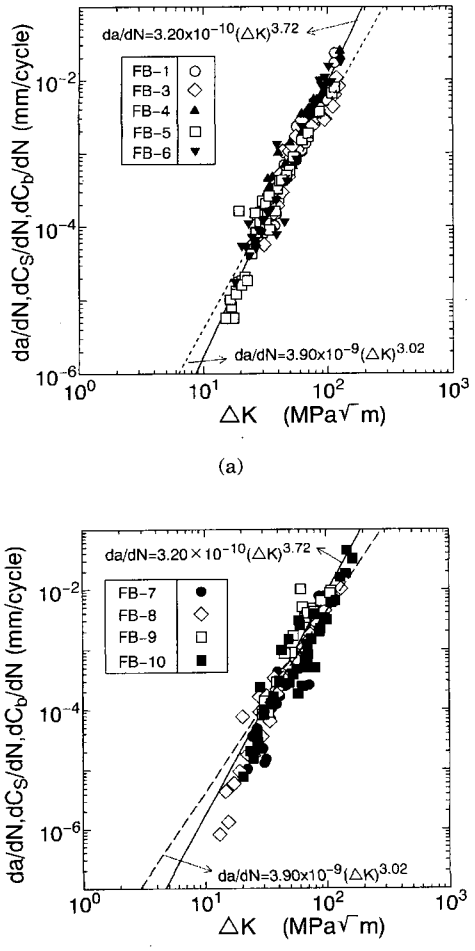

Fig. 6. Fatigue crack growth rate, *da/dN* and stress intensity factor range, *ΔK*.

the influence of crack initiation life. The relationship between the *da/dN* values obtained from the *N* vs crack length curves, and the *ΔK* obtained from Equations (3) and (4) and the Newman-Raju formula (Fig. 1(a)) is shown in Figures 6(a) and 6(b). These results suggest that the relationship between *da/dN* and *ΔK* can be expressed as Equation (6) regardless of the initial crack shape and whether the measurement was carried out before or after penetration :

$$da/dN(mm/cycle)=3.20\times10^{-10}(\Delta K)^{3.72}(MPa\sqrt{m}) \quad (6)$$

All fatigue crack growth data are shown in Figure 6(a) and 6(b). In this figure, the open symbols represent crack growth rate of low bending stress specimens, and the solid symbols represent crack growth rate of specimens subjected to elastic-plastic bending stress. Before penetration ($da/dN \leq 10^{-3}$ $(mm/cycle)$, high stress and low stress specimens show similar *da/dN* values for the same *ΔK*. However after penetration, *da/dN* is higher for high stress specimens than for low stress specimens. The dotted lines in Figure 6(a) and 6(b) are a fatigue crack growth curve for *STS410* carbon steel pipes proposed by Kobayashi *et al.*[8] and can be expressed as the following equation :

$$da/dN(mm/cycle)=3.90\times10^{-9}(\Delta K)^{3.02}(MPa\sqrt{m}) \quad (7)$$

For the *da/dN* obtained from low bending stress specimens, Equation (7) is better than Equation (6). However, for the all *da/dN* data, Equation (6) can be a best fit curve.

Before penetration, the crack shapes and the *N* vs a curves were calculated using the fatigue crack propagation Equation (6) and the Newman-Raju formula. The lines in Figure 3 show the calculated aspect ratios, which reveal a good agreement with the experimental ones. The correlation between the calculated leak life N_L and the experimental one is illustrated in Figure 7. Although the maximum error is 84.7 % and most experimental data are greater than the calculated data, they also show a good agreement. After crack penetration, the outer and inner half crack length C_S and C_b vs the number of cycles were calculated and plotted in Figure 8 by using the proposed *K* equations

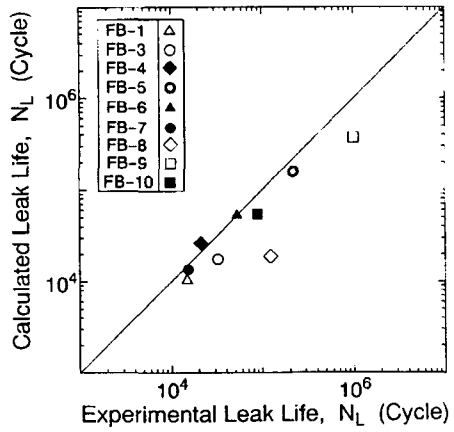

Fig. 7. Comparison between experimental leak life N_L and calculated leak life N_L.

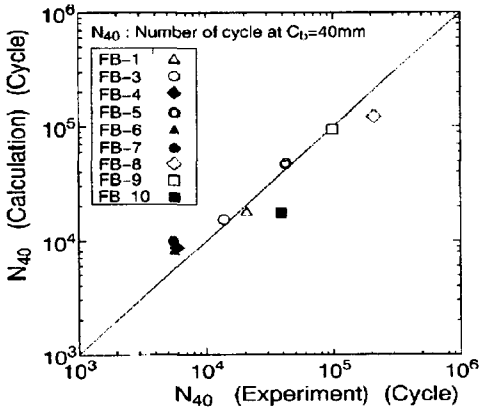

Fig. 9. Comparison between experimental and calculated N_{40} after penetration.

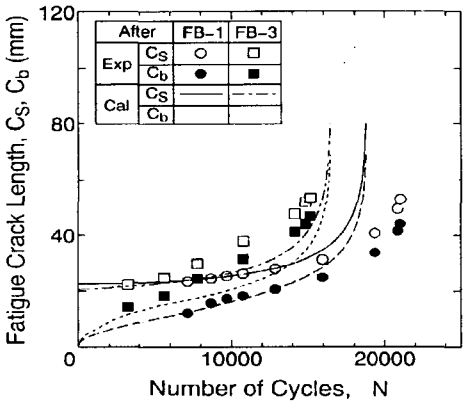

Fig. 8. Comparison between experimental and calculated crack growth behavior after penetration.

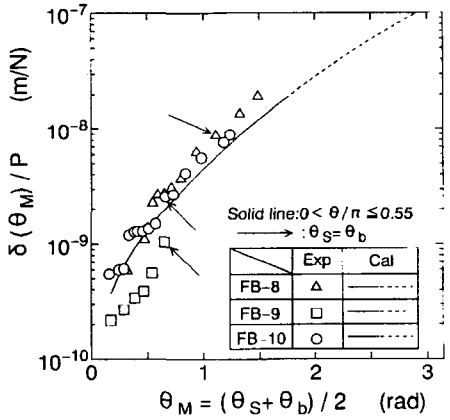

Fig. 10. Comparison between experimental and calculated crack opening displacement.

(Eq. 3, 4) and fatigue crack growth equation (Eq. 6).

The correlation between the calculated and experimental values of N_{40} is shown in Figure 9. From this figure, it can be seen that the calculated N_{40} shows good agreement with the experimental N_{40}. For this case, the maximum error is 54 %.

Crack opening displacements were measured by a clip gauge at 3 *mm* inside from outer surface of maximum tensile stress point and calculated by Equation (2). The crack opening displacements per load($\delta(\theta_M)/P$) as a function of θ_M illustrated in Figure 10 represent a quite agreement between the experimental and calculated values.

CONCLUSIONS

1. A new equation was proposed for evaluating K before and after crack penetration in a pipe subjected to bending load.

2. Before crack penetration, crack growth behavior such as aspect ratio and leak life was evaluated successfully using the Newman-Raju equation and the plate model proposed.
3. After crack penetration, crack growth behavior such as crack shape, fatigue life and crack opening displacement were evaluated quantitatively by using the equation and pipe model proposed in this paper.

REFERENCES

1) Fujitani, T. et al.(1988) : SPB liquefied gas carrier 'Kayoh Maru', Ishikawajima-Harima Engng Rev.(IHI) 28, 380−386 (in Japanese).
2) ASME(1995) Boiler and Pressure Vessel Code Sec. XI.
3) Hasegawa, K. *et al.* (1983) : Prediction of fracture tolerances for stainless steel pipes with circumferential crack, ASME Int. J. Press. Ves. and Piping 95, 65−78.
4) Nam, K.W. et al. (1992) : Leak-before-break conditions of plates and pipes under high fatigue stresses, Fatigue Fract. Engng Mater. Struct 15, 809−824.
5) Bergman, M. (1995) : Stress intensity factors for circumferential surface cracks in pipes, Fatigue Fract. Engng Mater. Struct. 18, 1155−1172.
6) Newman, J.C., Jr. and Raju, I.S. (1981) : An empirical stress intensity factor equation for the surface crack, Engng. Fract. Mech. 15, 185-192.
7) Zahoor, A. (1989) : Ductile Fracture Handbook 3, Novetech Corporation and Electric Power Research Institute.
8) Kobayashi, H. *et al.* (1989) : Construction of a fatigue crack growth data base for nuclear component ferritic steels in Japan and its statistical analysis, Trans. Japan Soc. Mech. Eng. 55, 1255−1263 (in Japanese).